Fermi National Accelerator Laboratory

Fermilab-Conf-86/135-T September, 1986

The Effects of Resonant Neutrino Oscillations on the Solar Neutrino Experiments[1]

Stephen J. Parke

Fermi National Accelerator Laboratory

P.O. Box 500, Batavia, Illinois, 60510

Abstract

Analytic results are derived for the electron neutrino survival probability after passage through a resonant oscillation region. This survival probability together with a sophisticated model of the production distribution of the solar neutrino sources and the solar electron number density are used to study the effects of resonant neutrino oscillation in the solar interior on the current and proposed solar electron neutrino experiments.

---

[1]Invited talk at the Workshop on Quarks and Galaxies, Berkeley, July 28-August 15,1986

Operated by Universities Research Association Inc. under contract with the United States Department of Energy

The Effects of Resonant Neutrino Oscillations on the Solar Neutrino Experiments[1]

Stephen J. Parke

Fermi National Accelerator Laboratory

P.O. Box 500, Batavia, Illinois, 60510

Abstract

Analytic results are derived for the electron neutrino survival probability after passage through a resonant oscillation region. This survival probability together with a sophisticated model of the production distribution of the solar neutrino sources and the solar electron number density are used to study the effects of resonant neutrino oscillation in the solar interior on the current and proposed solar electron neutrino experiments.

Recently, Mikheyev and Smirnov[1] have shown that the matter neutrino oscillations of Wolfenstein[2] can undergo resonant amplification in the solar interior thereby reducing the flux of electron neutrinos emerging from the Sun. This mechanism may be the solution to the solar neutrino puzzle[3,4]. Subsequently, Bethe[5] and others[6] have refined and restated the Mikheyev and Smirnov idea, pointing out that there are three general regions of parameter space in which the solar electron neutrino flux is sufficiently reduced. In this paper, I report an analytic result[7] for the electron neutrino survival probability after passage through a resonant oscillation region. Then, I outline a calculation[8] which uses this result, together with a relatively sophisticated solar model for the production distribution of solar neutrino sources and the solar electron number density, to generate contour plots of electron neutrino capture rates in the mass difference squared - vacuum mixing angle plane, for both chlorine (^{37}Cl) experiment and the proposed gallium (^{71}Ga) detector.

If neutrinos are massive then the flavor and mass eigenstates are not necessarily identical, however a general neutrino state can always be written in the

flavor basis[9],

$$|\nu(t)\rangle = c_e(t)\,|\nu_e\rangle + c_x(t)\,|\nu_x\rangle\,. \tag{1}$$

In the ultra-relativistic limit, the evolution of this general neutrino state, in matter, is described by the following Schrodinger-like equation[3],

$$i\frac{d}{dt}\begin{pmatrix} c_e \\ c_x \end{pmatrix} = \frac{\Delta_N}{2}\begin{pmatrix} -\cos 2\theta_N & \sin 2\theta_N \\ \sin 2\theta_N & \cos 2\theta_N \end{pmatrix}\begin{pmatrix} c_e \\ c_x \end{pmatrix}. \tag{2}$$

With Δ_N and θ_N determined by

$$\Delta_N \cos 2\theta_N = \frac{\delta m^2}{2k}\cos 2\theta_0 - \sqrt{2}G_F N_e,$$

$$\Delta_N \sin 2\theta_N = \frac{\delta m^2}{2k}\sin 2\theta_0$$

where $\delta m^2 \equiv (m_2^2 - m_1^2)$, m_i are the neutrino masses, k is the neutrino energy, θ_0 is the vacuum mixing angle, G_F is the Fermi constant and N_e is the electron number density. The constraints $\delta m^2 > 0$ and $\theta_0 < \pi/4$ are assumed.

At an electron density, N_e, the matter mass eigenstates are

$$|\nu_1, N\rangle = \cos\theta_N\,|\nu_e\rangle - \sin\theta_N\,|\nu_x\rangle$$

$$|\nu_2, N\rangle = \sin\theta_N\,|\nu_e\rangle + \cos\theta_N\,|\nu_x\rangle \tag{3}$$

which have eigenvalues $E_1 = -\Delta_N/2$ and $E_2 = \Delta_N/2$. At resonance, the electron density is given by $N_e^{res} = \delta m^2 \cos 2\theta_0/2\sqrt{2}kG_F$, and the matter mixing angle $\theta_N^{res} = \pi/4$. Above resonance, θ_N satisfies $\pi/4 < \theta_N \leq \pi/2$.

For a constant electron density these matter mass eigenstates evolve in time by the multiplication of a phase factor. Also, for a slowly varying electron density, these states evolve independently in time; i.e. $e^{-i\int^t E_1 dt}\,|\nu_1, N(t)\rangle$ and $e^{-i\int^t E_2 dt}\,|\nu_2, N(t)\rangle$ are the adiabatic states. Therefore, it is convenient to use these states, as the basis states, in the region for which there are no transitions (away from the resonance region). As a neutrino goes through resonance these adiabatic states maybe mixed, but on the other side of resonance, the neutrino state can still be written as a linear combination of these states. That is, a basis state produced at time t, going through resonance at time t_r, and detected at time t' is described by

$$e^{-i\int_t^{t_r} E_1 dt}\,|\nu_1, N(t)\rangle \rightarrow$$

$$a_1\, e^{-i\int_{t_r}^{t'} E_1 dt}\,|\nu_1, N(t')\rangle + a_2\, e^{-i\int_{t_r}^{t'} E_2 dt}\,|\nu_2, N(t')\rangle$$

or

$$e^{-i\int_{t_r}^{t} E_2 dt}\ |\nu_2, N(t)\rangle \rightarrow$$

$$-a_2^*\ e^{-i\int_{t_r}^{t'} E_1 dt}\ |\nu_1, N(t')\rangle\ +\ a_1^*\ e^{-i\int_{t_r}^{t'} E_2 dt}\ |\nu_2, N(t')\rangle$$

where a_1 and a_2 are complex numbers such that $|a_1|^2 + |a_2|^2 = 1$. The relationship between the coefficients, for these two basis states, is due to the special nature of the wave equation, eqn(2). The phase factors have been chosen so that coefficients a_1 and a_2 are characteristics of the transitions at resonance and are not related to the production and detection of the neutrino state.

The detection averaged electron neutrino survival probability is easily calculated as

$$\begin{aligned} P_{\nu_e}(t) &= \frac{1}{2} + \frac{1}{2}(|a_1|^2 - |a_2|^2)\cos 2\theta_N \cos 2\theta_0 \\ &- |a_1 a_2| \sin 2\theta_N \cos 2\theta_0 \cos\left(\int_{t_r}^{t} \Delta_N dt + \omega\right) \end{aligned}$$

with $\omega = \arg(a_1 a_2)$. The last term shows that the phase of the neutrino oscillation at the point the neutrino enters resonance can substantially effect this probability. Therefore, we must also average over the production position, to obtain the fully averaged electron neutrino survival probability[7,10] as

$$\overline{P_{\nu_e}} = \frac{1}{2} + \left(\frac{1}{2} - P_x\right)\cos 2\theta_N \cos 2\theta_0 \qquad (4)$$

where $P_x = |a_2|^2$, the probability of transition from $|\nu_2, N>$ to $|\nu_1, N>$ (or vice versa) during resonance crossing. The non-resonant crossing case is trivially obtained by setting $P_x = 0$.

To calculate the probability, P_x, the approximation that the density of electrons varies linearly in the transition region is used. That is, a Taylor series expansion is made about the resonance position and the second and higher derivative terms are discarded. In this approximation the probability of transition between adiabatic states was calculated by Landau and Zener. This is achieved by solving the Schrodinger equation, eqn(2), exactly in this limit. Applying their result to the current situation[7,11] gives

$$P_x = \exp\left[-\frac{\pi}{2}\frac{\sin^2 2\theta_0}{\cos 2\theta_0}\frac{\delta m^2/2k}{|\vec{n}\cdot\nabla \ln N_e|_{res}}\right] \qquad (5)$$

where the unit vector, $\vec{n}$, is in the direction of propagation of the neutrino. Eqn(4) and (5) demonstrate that only the electron number density, at production, and the logarithmic derivative of this density, at resonance, determine the electron neutrino survival probability. For a discussion of the range of validity of this approximation see ref(7).

Before applying these results to the solar model in detail, let us first consider an exponential electron number density profile which is a good approximation for the solar interior except near the center. In figure (1), I have plotted the electron neutrino survival probability contours at the earth in the $\delta m^2/2\sqrt{2}kG_F N_c$ versus $\sin^2 2\theta_0/\cos 2\theta_0$ plane for such an exponential density profile. Here, the Solar central electron number density, N_c, is also the number density at the point where the neutrinos are produced. This plot depends only on the properties of the sun and this dependency is through the combination $R_e N_c$, where R_e is the scale height. For this figure, I have used an N_c corresponding to a density of 140g cm^{-3} and $Y_e = 0.7$ and a scale height R_e of 0.092 times the radius of the sun.

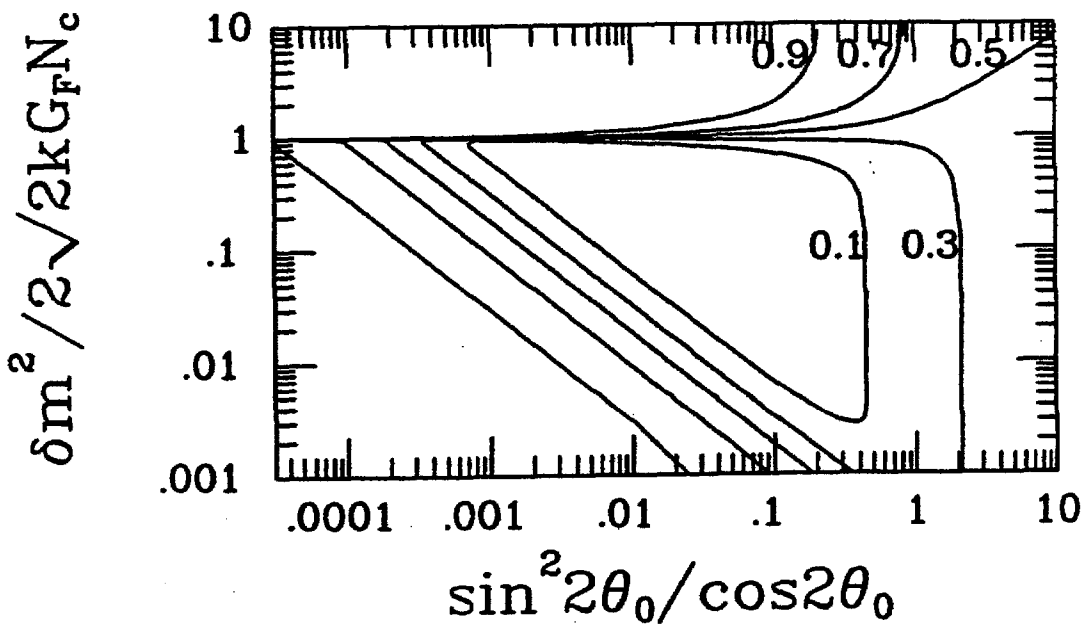

Fig. (1): Electron neutrino survival probability contours for an exponential solar electron density profile and an electron neutrino produced at the center of the Sun.

Above the line $\delta m^2/2\sqrt{2}kG_F N_e = 1/\cos 2\theta_0$ in this plot, the neutrinos never cross the resonance density on there way out of the sun. Here, the probability of detecting an electron neutrino is close to the standard neutrino oscillation result. Below this line, the effects of passing through resonance comes into play. Inside the 0.1 contour "triangle", there is only a small probability of transitions between the adiabatic states as the neutrino passes through resonance. To the right of this contour triangle, the probability of detecting a neutrino grows, not because of transitions, but because both adiabatic states have a substantial mixture of electron neutrino at zero density. To the left and below the 0.1 contour triangle, the probability grows because here there are significant transitions between the adiabatic states as the neutrino crosses resonance.

More precisely, the solar electron neutrino capture rate for a detector characterized by a electron neutrino capture cross section, σ(E), and energy threshold E_0, is

$$\sum_{\text{processes}} \int_{E_0}^{\infty} \frac{d\Phi_\nu}{dE} \sigma(E) dE. \tag{6}$$

The sum is taken over all neutrino sources in the Sun and $d\Phi_\nu/dE$ is the differential electron neutrino flux of a given source at the earth's surface. To include the reduction in the electron neutrino flux from the Sun due to resonant neutrino oscillations, the differential electron neutrino flux for each process was calculated as

$$\frac{d\Phi_\nu}{dE} \propto W(E) \int_{\text{sun}} dV \; \overline{P_{\nu_e}} \frac{df}{dV} \tag{7}$$

where W(E) is the standard weak interaction energy distribution for the neutrinos of a given process and df/dV is the fraction of the standard solar model flux coming from a given solar volume element for this process. The solar electron number density profile, $\rho Y_e/m_N$, and the values of df/dV for the various processes were taken from Bahcall's solar model[12], see figure (2). We have assumed that the spatial distributions for pep and CNO neutrinos are given by those for pp and ^{8}B neutrinos, respectively[13]. We normalize $d\Phi_\nu/dE$ for each process by demanding that the energy and solar volume integrations of eqn.(6) yield the capture rates quoted by Bahcall when $\overline{P_{\nu_e}} = 1$.

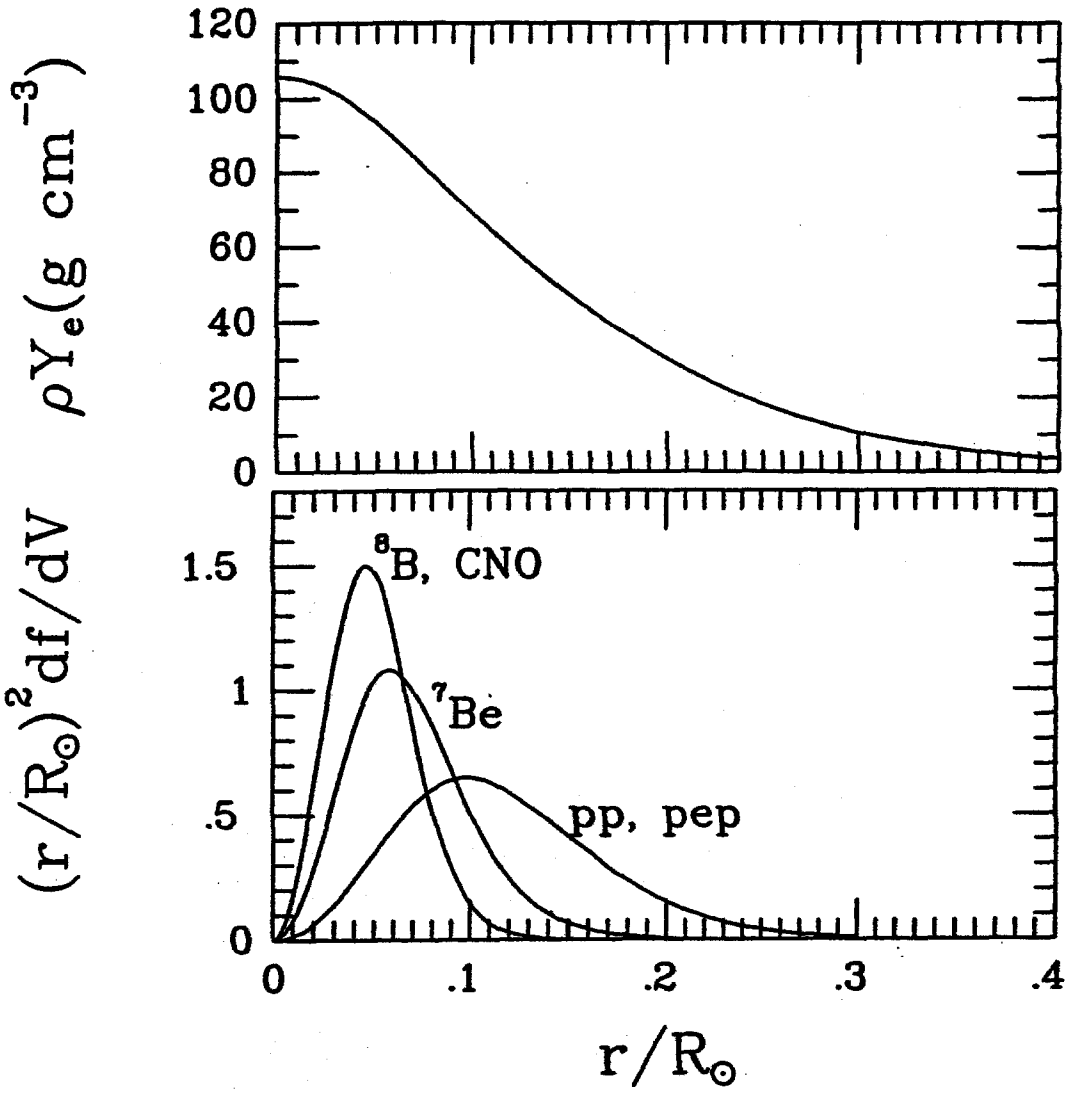

Fig. (2):Electron number density and the fractional neutrino emissivity per shell verus the radial distance from the solar center.

The cross sections, σ(E), used for the ^{37}Cl and ^{71}Ga detectors, whose thresholds are 814 and 236 keV respectively, are given in figure (3). The ^{37}Cl cross section is derived from the data of Bahcall[12] and the ^{71}Ga cross section is a fit to the low energy calculation of Bahcall[14] and the higher energy calculations of Grotz, Klapdor, and Metzger[15]. In Table I, we list two sets of expected capture rates for both the chlorine and gallium experiments and the maximum neutrino energy for each solar neutrino source. Model A is taken from the values of Bahcall *et al.*[4] and Model B, reported by Bahcall[16], reflects recent changes in the expected solar neutrino capture rate. The most important change being in the

estimation of the Sun's opacity which alters the solar temperature profile. A comparison between these two models demonstrates the insensitivity of the allowed region of parameter space to small changes in the solar model. The value of 16 SNU for the ^{8}B rate in Model A for the gallium experiment is an average of the new predictions of Grotz *et al.*and Mathews *et al.*[17].

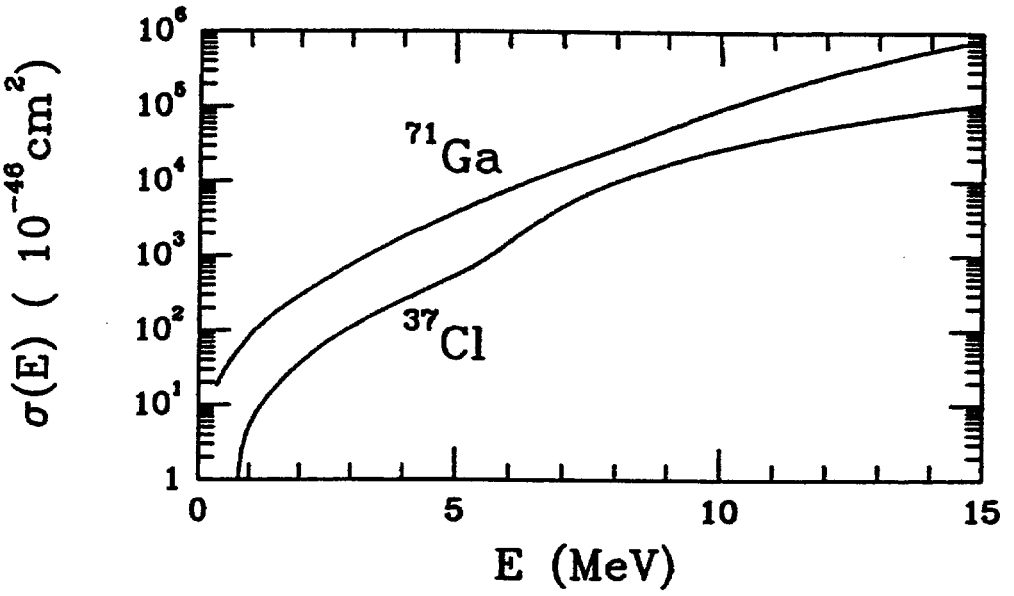

Fig. (3): The cross sections for the Chlorine and Gallium detectors as a function of energy.

Table I: Neutrino Sources and Capture Rates for Two Solar Models

Process	E_ν^{max}(MeV)	Chlorine (SNU)		Gallium (SNU)	
		Model A	Model B	Model A	Model B
^{8}B	14.06	4.3	5.75	16.0	18.0
^{7}Be	0.861(90%)				
	+ 0.383(10%)	1.0	1.1	27	34
p-p	0.420	0	0	70	70
pep	1.44	0.23	0.20	2.5	3.0
^{13}N	1.199	0.08	0.10	2.6	4.0
^{15}O	1.732	0.26	0.35	3.5	6.0
Total		5.9	7.5	122	135

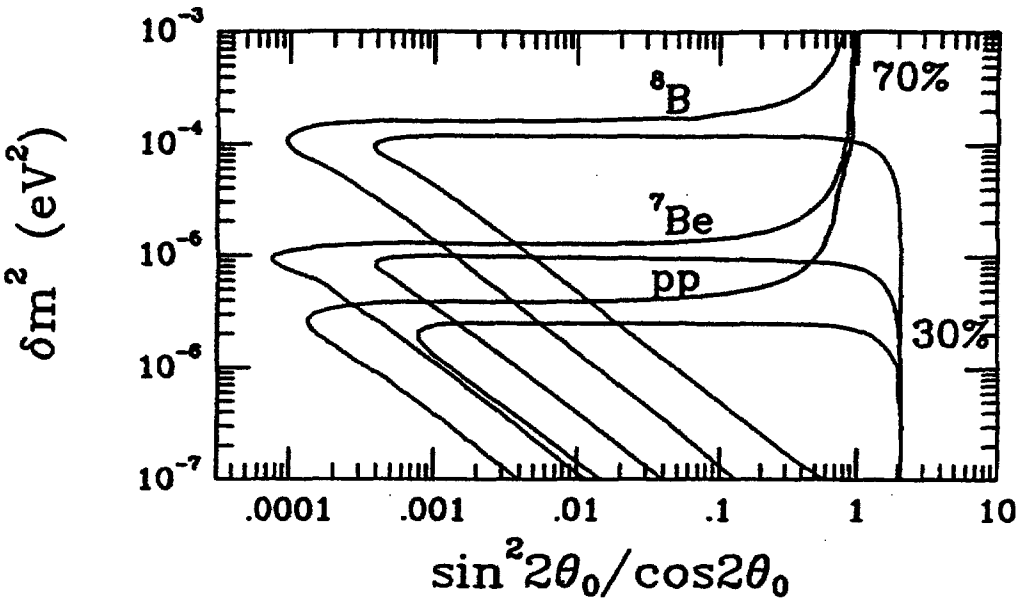

Fig. (4): The 70% and 30% electron neutrino rate contours for the principal solar neutrino sources in the Gallium experiment.

From Table I we can see that the ^{8}B, ^{7}Be and pp neutrinos account for about 90% of the capture rate for both the ^{37}Cl and ^{71}Ga experiments. Therefore by understanding the effect of resonant neutrino oscillation on these processes we can understand the effect on both of these experiments. In figure (4) I have plotted the 30% and 70% electron neutrino capture rate contours for the Gallium experiment for the three main types of neutrinos emitted from the Sun. For the Chlorine experiment the ^{8}B and ^{7}Be contours are indistinguishable from those in figure (4) because of the similarity of the cross sections energy dependence for these experiments. The total electron neutrino capture rates are obtained by an appropiately weighted superposition of these contours.

In figures 5 and 6, we present electron neutrino capture rate contours (iso-SNU contours) for the ^{37}Cl and ^{71}Ga experiments as a function of δm^2 and $\sin^2 2\theta_0/\cos 2\theta_0$ for the two solar models discussed earlier. The 1σ deviations from the Davis *et al.*[3] result of 2.1 SNU are the 2.4 and 1.8 iso-SNU contour lines in fig. 5 The similarity of the shape of these plots for the two solar models reflects the insensitivity of the resonant oscillation process to small changes in the structure of the Sun. However, the position of individual contours does change, due to changes in the contributions from the individual neutrino sources.

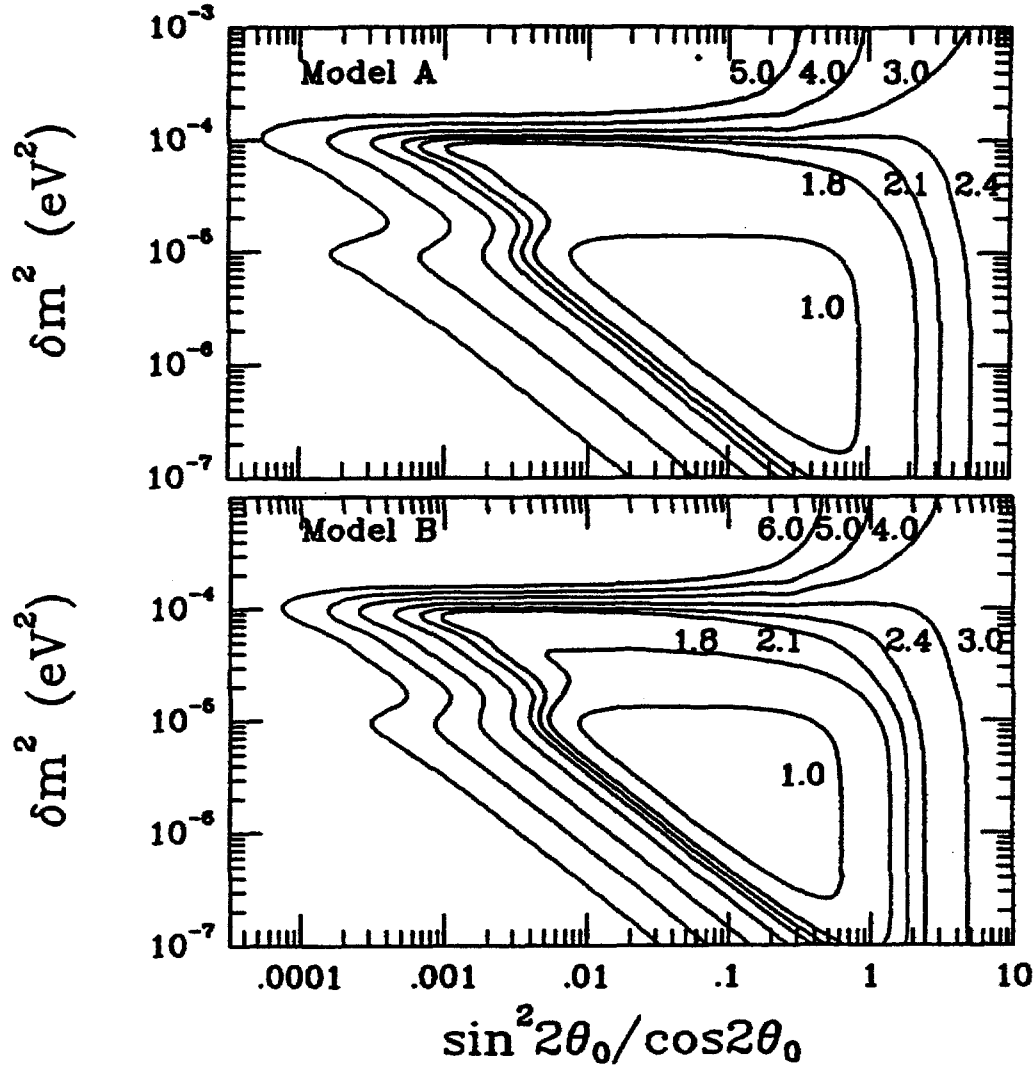

Fig. (5): Iso-SNU contours for the ^{37}Cl experiment for the solar models listed in Table I. The contours are labeled with their the corresponding SNU values.

The generic structure of these total SNU plots is due to the superposition of triangular iso-SNU contours associated with each individual neutrino source contributing to a given total SNU value. These individual contours owe their shape to the appropriate iso-probability contour, figure (1), and their position is determined by the typical energy scale and production electron density of the individual neutrino source, figure (4). For each neutrino source the resonance mechanism becomes important, provided $\theta_0 > 0.01$, as soon as δm^2 becomes small enough so that the average resonant electron density for that source is

less than the solar electron density at the production site. This occurs when δm^2 is approximately equal to 1.5×10^{-4}, 1.2×10^{-5}, and 3.7×10^{-6} eV^2 for the ^8B, ^7Be and pp neutrinos respectively. Below these values the individual neutrino sources have contours which are diagonals of slope minus one coming from the form of the transition probability between adiabatic states, eqn(5). The intersection of these diagonal lines with the turning on of resonance for ^8B, ^7Be and pp is responsible for the shoulders at small $\sin^2 2\theta_0/\cos 2\theta_0$ in the contour plots. The vertical sections of the contours, at large θ_0, occurs because for large θ_0 both adiabatic states have a large component of electron neutrino.

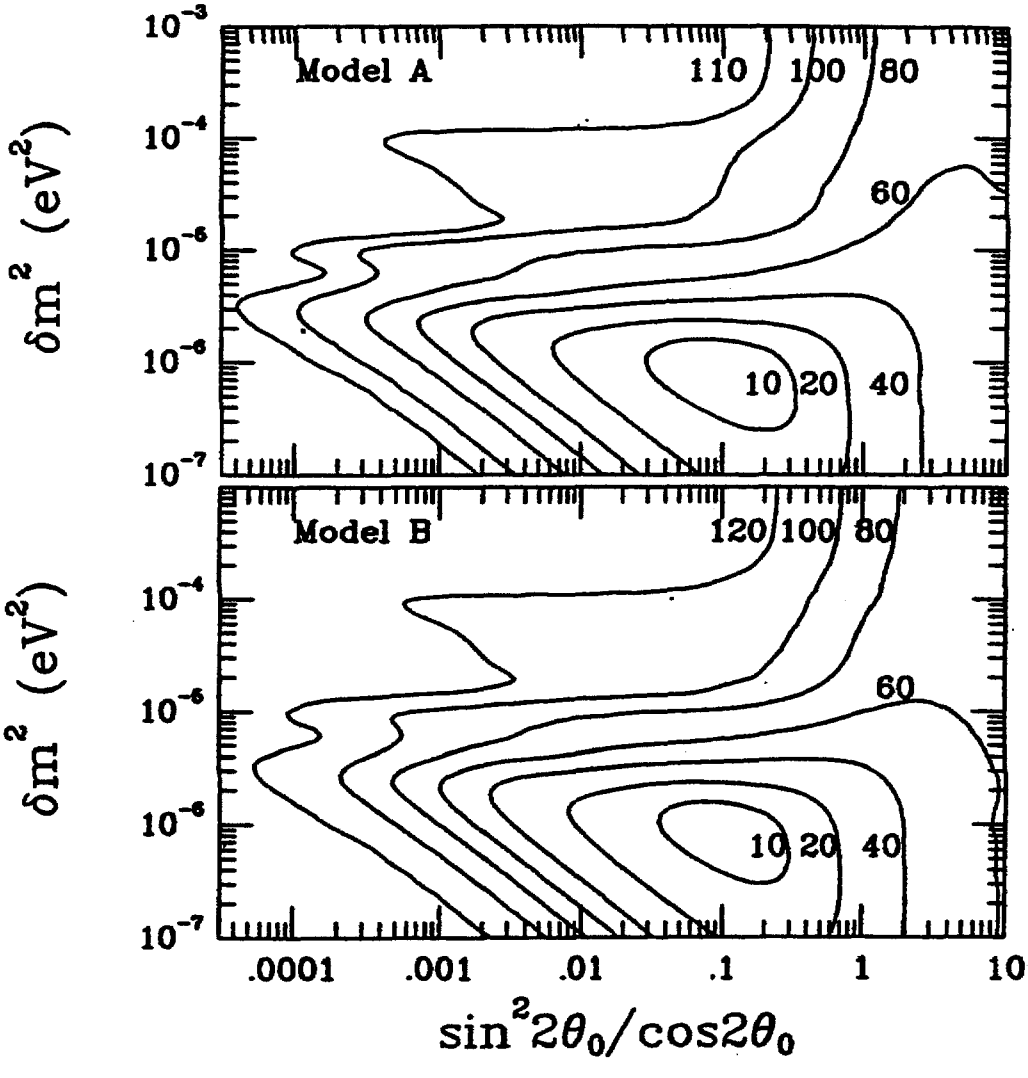

Fig. (6): Iso-SNU contours for a ^{71}Ga detector for the solar models listed in Table I. The contours are labeled with their the corresponding SNU values.

From fig. 6, we see that the results of the ^{71}Ga experiment can range from 10 to 120 SNU and still be compatible with the ^{37}Cl experiment. In general, a given gallium contour crosses the 2.1 $\pm$ 0.3 chlorine contour at least twice and therefore the results of the ^{71}Ga experiment will leave a two-fold degeneracy in (δm^2, θ_0)-space. If one accepts the theoretical prejudice against large vacuum angles provided by see-saw models[18], this degeneracy is removed. Unfortunately, the degeneracy is continuous for that region of parameter space corresponding to a ^{37}Cl rate of 2.1 $\pm$ 0.3 SNU and a ^{71}Ga rate greater than 100 SNU. In this region *only* the ^{8}B neutrinos are effected by the resonance phenomena. Also, in this region of parameter space the two experiments will not be able to distinguish between a small temperature change at the solar core and the resonant neutrino oscillation mechanism. This is due to the relatively strong temperature dependence of the ^{8}B neutrino flux[19]. It is only when the ^{71}Ga SNU rate is depleted below that of merely removing the ^{8}B component (*i.e.*, appreciably less than 110 SNU), so that reduction of the less temperature sensitive neutrinos (^{7}Be and pp) becomes necessary, that the resonant oscillation mechanism becomes a likely solution to the solar neutrino problem.

Many thanks go to my collaborator Terry Walker.

Fermilab is operated by Universities Research Association Inc. under contract with the United States Department of Energy.

References

1. S.P. Mikheyev and A.Yu. Smirnov, *10th International Workshop on Weak Interactions and Neutrinos*, Savonlinna, Finland(1985); *Nuovo Cimento* C9, 17(1986).

2. L. Wolfenstein, *Phys. Rev.* D17, 2369(1978); *Phys. Rev.* D20, 2634(1979).

3. R. Davis, D.S. Harmer, and K.C. Hoffman, *Phys. Rev. Lett.* 20, 1205(1968).

4. J.N. Bahcall, B.T. Cleveland, R. Davis, and J.K Rowley, *Astrophys. J.* 292, L79(1985).

5. H.A. Bethe, *Phys. Rev. Lett.* **56**, 1305(1986).

6. A. Messiah and S.P. Rosen and M. Spiro, *1986 Massive Neutrinos in Astrophysics and in Particle Physics*, Tignes, January 1986; S.P. Rosen and J.M. Gelb, *Phys. Rev.* , **D34**, 969(1986); E.W. Kolb, M.S. Turner, and T.P. Walker, Phys. Lett., **B175**, 478(1986); V. Barger, R.J.N. Phillips, and K. Whisnant, *Phys. Rev.* , D34, 980(1986); J. Bouchez, M. Cribier, J. Rich, M. Spiro, D. Vignard and W. Hampel, DPhPE 86-10, May 1986.

7. S.J. Parke, *Phys. Rev. Lett.* **57**, 1275(1986).

8. S.J. Parke and T.P. Walker, *Phys. Rev. Lett.* (to be published).

9. The other flavor eigenstate could ν_μ or ν_τ.

10. A. Messsiah, see ref. 6.

11. W.C. Haxton, *Phys. Rev. Lett.* **57**, 1271(1986).

12. J.N. Bahcall, W.F. Huebner, S.H. Lubow, P.D. Parker, and R.K. Ulrich, *Rev. Mod. Phys.* **54**, 767(1982).

13. The CNO distributions are undoubtedly tighter than ^{8}B due to their more sensitive dependence on temperature, but the inaccuracy introduced by this approximation is negligible.

14. J.N. Bahcall, in *Proceedings of the Neutrino Mass Miniconference*, eds. V. Barger and D. Cline, Telemark, Wisconsin(1980).

15. K. Grotz, H.V. Klapdor, and J. Metzinger, *Astron. Astrophys.* **154**, L1(1986).

16. J. N. Bahcall, *International Symposium on Weak and Electromagnetic Interactions in Nuclei*, Heidelberg, July 1986.

17. G.J. Mathews, S.D. Bloom, G.M. Fuller, and J.N. Bahcall, *Phys. Rev.* , **C32**, 796(1985).

18. T. Yanagida, *Prog. Theor. Phys.* **B135**, 66(1978); M. Gell-Mann, P. Ramond, and R. Slansky, in *Supergravity*, eds. P. van Nieuwenhuizen and D. Freedman, (North Holland)(1979).

19. In the case where a ^{71}Ga rate of $\gtrsim$ 100 SNU is measured, a measurement of the ^{8}B solar neutrino spectrum (see Rosen and Gelb ref. 6) or the flavor independent solar neutrino spectrum (see S. Weinberg, *XXIII International Symposium on High Energy Physics*, Berkeley, July 1986) would allow us to distinguish between changes in the solar model and resonant neutrino oscillations.